Hierarchy and Roles of Pathogen-Associated Molecular Pattern-Induced Responses in *Nicotiana benthamiana*[1][W]

Cécile Segonzac, Doreen Feike[2], Selena Gimenez-Ibanez[3], Dagmar R. Hann[4], Cyril Zipfel, and John P. Rathjen[5]*

Sainsbury Laboratory, Norwich NR4 7UH, United Kingdom

Our current understanding of pathogen-associated molecular pattern (PAMP)-triggered immunity signaling pathways in plants is limited due to the redundancy of several components or the lethality of mutants in Arabidopsis (*Arabidopsis thaliana*). To overcome this, we used a virus-induced gene silencing-based approach in combination with pharmacological studies to decipher links between early PAMP-triggered immunity events and their roles in immunity following PAMP perception in *Nicotiana benthamiana*. Two different calcium influx inhibitors suppressed the reactive oxygen species (ROS) burst: activation of the mitogen-activated protein kinases (MAPKs) and PAMP-induced gene expression. The calcium burst was unaffected in plants specifically silenced for components involved in ROS generation or for MAPKs activated by PAMP treatment. Importantly, the ROS burst still occurred in plants silenced for the two major defense-associated MAPK genes *NbSIPK* (for salicylic acid-induced protein kinase) and *NbWIPK* (for wound-induced protein kinase) or for both genes simultaneously, demonstrating that these MAPKs are dispensable for ROS production. We further show that *NbSIPK* silencing is sufficient to prevent PAMP-induced gene expression but that both MAPKs are required for bacterial immunity against two virulent strains of *Pseudomonas syringae* and their respective nonpathogenic mutants. These results suggest that the PAMP-triggered calcium burst is upstream of separate signaling branches, one leading to MAPK activation and then gene expression and the other to ROS production. In addition, this study highlights the essential roles of *NbSIPK* and *NbWIPK* in antibacterial immunity. Unexpectedly, negative regulatory mechanisms controlling the intensity of the PAMP-triggered calcium and ROS bursts were also revealed by this work.

Plant immunity relies on two levels of pathogen perception that trigger defense mechanisms (Jones and Dangl, 2006). The first involves the recognition of conserved microbial elicitors termed pathogen-associated molecular patterns (PAMPs) by specific plasma membrane receptors. The receptors activate signaling cascades that trigger transcriptional and physiological changes within the host cell, ultimately restricting pathogen growth (Boller and Felix, 2009). Adapted pathogens have evolved the ability to inject effector proteins inside the host cell to counteract PAMP-triggered immunity (PTI), a prerequisite for their multiplication. However, a second branch of plant immunity based on internal recognition of effector proteins by cytoplasmic receptors has evolved, and it initiates stronger defense responses (Jones and Dangl, 2006). Both branches of plant immunity share common signaling messengers such as calcium ions (Ca^{2+}), reactive oxygen species (ROS), and mitogen-activated protein kinase (MAPK) cascades and lead to the reinforcement of cell walls, the production of antimicrobial metabolites, and in some case the programmed death of infected cells called the hypersensitive response (Lorrain et al., 2003; Boller and Felix, 2009).

Current knowledge of signaling events during PTI is derived largely from studies on the model species Arabidopsis (*Arabidopsis thaliana*), where two major PAMP receptors are known. The receptor kinase FLAGELLIN SENSING2 (FLS2) recognizes the active epitope flg22 of the bacterial flagellin, whereas the related molecule EF-Tu RECEPTOR binds the bacterial elongation factor Tu (Gómez-Gómez and Boller, 2000; Kunze et al., 2004; Chinchilla et al., 2006; Zipfel et al., 2006). Two further protein kinases, BRI1 ASSOCIATED KINASE1 (BAK1) and BOTRYTIS-INDUCED KINASE1, are positive regulators of these PAMP receptors (Chinchilla et al., 2007; Heese et al., 2007; Lu et al., 2010; Zhang et al., 2010). Forward genetics screens uncovered the PAMP receptor genes and *BAK1* but appear to be saturated, because further efforts could only identify genes for transcriptional control or biogenesis of PAMP receptors (Li et al., 2009; Lu et al.,

[1] This work was supported by the Biotechnology and Biological Sciences Research Council (grant no. BB/E017134/1 to J.P.R.) and by the Gatsby Charitable Foundation (to C.Z. and J.P.R.).

[2] Present address: John Innes Centre, Norwich Research Park, Norwich NR4 7UH, UK.

[3] Present address: Centro Nacional de Biotecnologia, Campus de Cantoblanco, 28049 Madrid, Spain.

[4] Present address: Institute of Botany, University of Basel, Hebelstrasse 1, CH–4056 Basel, Switzerland.

[5] Present address: Research School of Biology, Australian National University, Canberra, ACT 0200, Australia.

* Corresponding author; e-mail john.rathjen@anu.edu.au.

The author responsible for distribution of materials integral to the findings presented in this article in accordance with the policy described in the Instructions for Authors (www. plantphysiol.org) is: John P. Rathjen (john.rathjen@anu.edu.au).

[W] The online version of this article contains Web-only data.
www.plantphysiol.org/cgi/doi/10.1104/pp.110.171249

2009; Nekrasov et al., 2009; Saijo et al., 2009; Boutrot et al., 2010). Two explanations for the inability to uncover further PTI loci by mutagenesis are, first, that such mutations might be lethal and, second, that functional redundancy between members of multigenic families prevents their identification. One strategy for addressing the second possibility is the use of RNA-based gene-silencing approaches, which can knock down the expression of multiple related genes (Small, 2007).

Early studies using purified PAMPs on cell suspensions allowed the identification of signaling events that occur immediately after elicitation (Garcia-Brugger et al., 2006). First, there are massive ions fluxes across the plasma membrane. The most prominent is an influx of Ca^{2+} from the apoplast, which causes a rapid increase in the cytosolic Ca^{2+} concentration (Blume et al., 2000; Lecourieux et al., 2002). To date, there is no genetic evidence concerning the identity of the channels that are responsible for the Ca^{2+} burst, mainly because the candidate genes, Glu receptors and cyclic nucleotide-gated channels (CNGCs), which belong to multigenic families, encode proteins that are able to form functional heteromultimers (White et al., 2002; Talke et al., 2003; Ma et al., 2009b). However, pharmacological studies on tobacco (*Nicotiana tabacum*) cells elicited with cryptogein, an elicitin from the oomycete pathogen *Phytophthora cryptogea*, have shown that the Ca^{2+} influx was necessary for various defense signaling events (Tavernier et al., 1995; Lecourieux et al., 2006).

Another hallmark event of PTI signaling is the rapid and transient production of reactive oxygen species (ROS), termed the ROS burst. These are thought to act in several ways: directly, as antimicrobial agents; as cross-linking components for the reinforcement of cell walls; and/or as secondary messengers during signal transduction (Torres, 2010). In Arabidopsis, the flg22-triggered ROS burst is controlled by the inducible respiratory burst oxidase homolog RbohD of the plasma membrane (Nühse et al., 2007; Zhang et al., 2007). In tobacco, ROS induced by cryptogein treatment requires the orthologous gene *NtRbohD* (Simon-Plas et al., 2002). In *Nicotiana benthamiana*, both *NbRbohA* and *NbRbohB* are required for ROS accumulation after treatment with *Phytophthora infestans* hyphal cell wall extracts (Yoshioka et al., 2003). The Rboh enzymes are synergistically regulated by Ca^{2+} binding to the EF-hand domains of their N-terminal cytosolic extension as well as by phosphorylation by Ca^{2+}-dependent protein kinases (CDPKs; Kobayashi et al., 2007; Ogasawara et al., 2008). Notably, RbohD is phosphorylated in response to flg22, and this phosphorylation is required for its activity (Benschop et al., 2007; Nühse et al., 2007).

Another important event in signal transduction downstream of PAMP perception is rapid activation of MAPK cascades, which are believed to be key components that regulate transcriptional changes in elicited cells. In Arabidopsis protoplasts, MPK6 and MPK3 are phosphorylated upon flg22 treatment and activate WRKY transcription factors (Nühse et al., 2000; Asai et al., 2002). In tobacco and *N. benthamiana*, the MPK6 and MPK3 orthologs, SIPK (for salicylic acid-induced protein kinase; Zhang and Klessig, 1998) and WIPK (for wound-induced protein kinase; Seo et al., 1995), are also activated rapidly after elicitation (Lebrun-Garcia et al., 1998; Dahan et al., 2009). Unfortunately, the lethality of MAPK multiple mutants is a major restriction for mechanistic studies. For example, attempts to generate loss-of-function MPK3 and MPK6 plants for phenotypic analysis have shown that the *mpk3 mpk6* double mutant was embryo lethal (Wang et al., 2007, 2008), thus preventing the detailed study of the role of these MAPKs in immunity.

To advance our understanding of the sequence of signaling events triggered by PAMP perception, we exploited *N. benthamiana* as an experimental system. This plant is highly amenable to transformation by *Agrobacterium tumefaciens* and knockdown of gene expression by virus-induced gene silencing (VIGS), allowing rapid manipulation of gene expression for in-depth analysis of plant-pathogen interactions (Goodin et al., 2008). *N. benthamiana* perceives several unrelated PAMPs, including bacterial flg22 and chitin, the major component of the fungal cell wall. Previously, we have identified and characterized the putative receptors for these two PAMPs (Hann and Rathjen, 2007; Gimenez-Ibanez et al., 2009). *NbFls2* is the ortholog of *AtFLS2*. *NbCerk1* shares high identity with *AtCERK1*, which encodes the Arabidopsis chitin receptor (Iizasa et al., 2010; Petutschnig et al., 2010).

In this study, we combined VIGS and pharmacological approaches in *N. benthamiana* to decipher links between early signaling events induced by flg22 and chitin and their roles in the defense response against pathogenic bacteria. Specific silencing of genes encoding some of the main pathway components, including *NbRbohB* and several MAPKs, coupled with the use of Ca^{2+} influx inhibitors allowed us to block individual PTI responses and relate these to transcriptional reprogramming and restriction of pathogen growth. These analyses indicated that the unrelated PAMPs trigger a similar order of events, although the kinetics of the responses varied. Two distinct branches of signaling occur downstream of the initial Ca^{2+} influx, one leading to ROS production and the other to the activation of MAPKs, transcriptional changes, and defense against bacteria. Unexpectedly, negative regulatory loops coordinating the intensity of the early events were also uncovered by this work.

RESULTS

Calcium Influx from Apoplastic Stores Is Required for the PAMP-Induced ROS Burst, MAPK Activation, and Gene Expression

The transient increase of cytosolic Ca^{2+} observed after PAMP elicitation is thought to constitute a major

signaling hub for downstream PTI events (Lecourieux et al., 2006; Jeworutzki et al., 2010). Only a few candidate Ca^{2+} channels that may participate in this process have so far been identified (Kadota et al., 2004; Ali et al., 2007; Ma et al., 2009a). Unfortunately, progress has been restricted by the redundancy between the members of these multigenic families (White et al., 2002; Talke et al., 2003). In this context, we used a pharmacological approach to study the role of the Ca^{2+} burst in PTI signaling pathways in *N. benthamiana*. The Ca^{2+} chelator EGTA and the Ca^{2+} channel blocker $LaCl_3$ have been used widely to study the Ca^{2+} burst (Tavernier et al., 1995; Lecourieux et al., 2002). Here, we created a *N. benthamiana* transgenic line (SLJR15) stably expressing the reporter protein Aequorin within the cytoplasm (Knight et al., 1993). To validate the system, we monitored the Ca^{2+} burst triggered upon treatment with the two unrelated PAMPs flg22 and chitin. Treatment with either PAMP caused an influx of Ca^{2+} ions visualized as an increase of Aequorin photon release over the 30-min period post elicitation (see *TRV*:*EV* control in Fig. 1C and Supplemental Fig. S1). As expected, both inhibitors and particularly $LaCl_3$ suppressed this influx in a dose-dependent manner. The presence of 5 mM EGTA in the assay solution suppressed 80% and 70% of the flg22- and chitin-induced Ca^{2+} bursts, respectively. At the same concentration, $LaCl_3$ was a more efficient inhibitor, suppressing 98% of the flg22- and chitin-induced Ca^{2+} bursts. Therefore, these inhibitors can be used to study PTI signaling events in the absence of the initial Ca^{2+} burst.

Several lines of evidence suggest that the Ca^{2+} burst is required to induce ROS production following elicitation (Lecourieux et al., 2002; Kobayashi et al., 2007). To test this in *N. benthamiana*, we measured flg22- and chitin-induced ROS production in the presence of increasing doses of EGTA or $LaCl_3$ (Fig. 1, A and B). The presence of 1 mM EGTA or 1 mM $LaCl_3$, which suppressed approximately 30% and approximately 70% of the total Ca^{2+} burst, respectively (Supplemental Fig. S1), was sufficient to inhibit more than 80% of the flg22- and chitin-induced ROS bursts (Fig. 1, A and B). This suggests the existence of a cytosolic Ca^{2+} concentration threshold required for ROS production upon PAMP treatment.

Certain Ca^{2+} channels can be activated by ROS (Mori and Schroeder, 2004). Therefore, we assayed the PAMP-triggered Ca^{2+} burst in SLJR15 plants silenced for the NADPH oxidase *NbRbohB* (*TRV*:*RbohB*) using a modified tobacco rattle virus (TRV) vector (Liu et al., 2002). *NbRbohB* was previously shown to be important for PAMP-induced ROS production (Yoshioka et al., 2003). As controls, we included plants silenced for the flagellin receptor *NbFls2* (*TRV*:*FLS2*; Hann and Rathjen, 2007), for the putative chitin receptor *NbCerk1* (*TRV*:*CERK1*; Gimenez-Ibanez et al., 2009), or for the empty vector (*TRV*:*EV*). The flg22- or chitin-induced Ca^{2+} burst was absent in Aequorin-expressing plants silenced for *NbFls2* or *NbCerk1*, respectively, demonstrating the

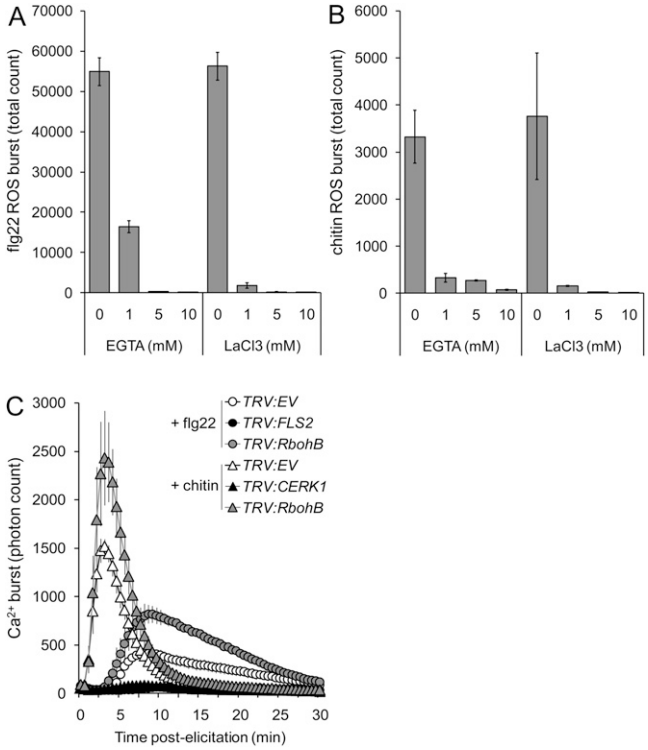

Figure 1. Apoplastic Ca^{2+} is required for the PAMP-triggered ROS burst. A and B, The Ca^{2+} chelator (EGTA) and the Ca^{2+} channel blocker ($LaCl_3$) inhibit flg22-induced (A) and chitin-induced (B) ROS bursts. ROS burst was measured in the *N. benthamiana* wild-type line. The samples were treated with increasing doses of EGTA or $LaCl_3$ together with the indicated PAMP. Data are presented as average sums of photon counts during a 60-min measurement for 12 samples ± SD. C, Flg22- and chitin-induced Ca^{2+} bursts occur and are enhanced by VIGS of *NbRbohB*. Ca^{2+} burst was measured in the *N. benthamiana* SLJR15 line silenced for the empty vector (*TRV*:*EV*), *NbFls2* (*TRV*:*FLS2*), *NbCerk1* (*TRV*:*CERK1*), or *NbRbohB* (*TRV*:*RbohB*). Data are presented as average signals of 12 samples ± SD.

specificity of this response (Fig. 1C). Silencing of *NbRbohB* completely abolished both the flg22- and chitin-induced ROS bursts (Supplemental Fig. S2). In the SLJR15 line silenced for *NbRbohB*, the Ca^{2+} burst observed in response to flg22 or chitin started at the same time as that observed in *TRV*:*EV* control plants, but surprisingly, its amplitude and duration were extended (Fig. 1C). These data indicate that the apoplastic stores of Ca^{2+} required for the PAMP-triggered Ca^{2+} burst are also essential for the activation of NbRbohB and consequent ROS production in *N. benthamiana*. These results further imply that ROS act as a negative regulator of the Ca^{2+} channels responsible for the PAMP-dependent Ca^{2+} influx.

MAPK activation is one of the earliest signaling events upon PAMP treatment (Nühse et al., 2000; Asai et al., 2002; Miya et al., 2007). To test if MAPK activation is Ca^{2+} dependent, we treated *N. benthamiana* leaf tissue with flg22 or chitin in the absence or presence of $LaCl_3$ and EGTA, then detected active MAPK forms by

western-blot analysis using an antibody that cross-reacts with the dually phosphorylated active form of the MAPK ERK1 (anti-pTEpY). First, the kinetics of MAPK activation by flg22 or chitin was investigated in wild-type *N. benthamiana* leaf samples treated with the elicitors for different amounts of time. As shown in Supplemental Figure S3, the signal detected with anti-pTEpY antibody appeared as early as 5 min following PAMP elicitation, peaked at 15 min, and returned to the basal level after 1 h. After 15 min, neither the Ca^{2+} channel blocker nor the Ca^{2+} chelator induced MAPK activation in the absence of PAMPs (Fig. 2A; Supplemental Fig. S4A). In this experiment, PAMP treatment caused the appearance of a single active MAPK (Fig. 2A; Supplemental Fig. S4A), which was later resolved into two forms (Supplemental Fig. S5). Cotreatment of leaf with $LaCl_3$ or EGTA strongly compromised MAPK activation by both flg22 and chitin. This suggests that the apoplastic Ca^{2+} required for the PAMP-triggered Ca^{2+} burst is also necessary for PAMP-dependent MAPK activation.

To further examine the link between Ca^{2+} influx and MAPK activation, we measured the PAMP-triggered Ca^{2+} burst in SLJR15 plants silenced for *NbSIPK* (*TRV*:*SIPK*), *NbWIPK* (*TRV*:*WIPK*), or both MAPKs together (*TRV*:*SW*; Asai et al., 2008). We first checked the reduction of transcript accumulation of the targeted genes in *TRV*:*SIPK*, *TRV*:*WIPK*, and *TRV*:*SW* silenced plants and correlated this with the MAPK signal detected by anti-pTEpY antibody (Supplemental Fig. S5). Quantitative reverse transcription (qRT)-PCR showed that the expression of *NbSIPK* was more than 90% reduced in *TRV*:*SIPK* and *TRV*:*SW* silenced plants while it was only slightly affected in *TRV*:*WIPK* silenced plants (Supplemental Fig. S5A). Similarly, the *NbWIPK* transcript was almost absent in *TRV*:*WIPK* and *TRV*:*SW* silenced plants (Supplemental Fig. S5B). These results demonstrate the efficiency and specificity of our VIGS system. In *TRV*:*EV* control plants, the anti-pTEpY antibody recognized two bands in leaf extracts after treatment with flg22 or chitin (Supplemental Fig. S5C). Silencing of either *NbFls2* or *NbCerk1* abolished the MAPK signal in the flg22- or chitin-treated samples, respectively. In *TRV*:*SIPK* silenced plants, only the lower band could be detected, whereas only the upper band was visible after elicitation in *TRV*:*WIPK* silenced plants. In *TRV*:*SW* silenced plants, both signals were strongly reduced or absent following elicitation. These results show that VIGS of *NbSIPK* and *NbWIPK* is functionally effective; that the upper band corresponds to NbSIPK and the lower band to NbWIPK; and that the expression of both MAPKs can be severely knocked down simultaneously in *TRV*:*SW* silenced plants.

We next tested whether the Ca^{2+} burst induced by PAMP treatment was compromised in plants silenced for MAPKs. As controls, we included *TRV*:*EV*, *TRV*:*FLS2*, and *TRV*:*CERK1* silenced plants. As shown previously, the flg22-induced Ca^{2+} burst was completely abolished in *TRV*:*FLS2* silenced plants (Fig. 2B). In

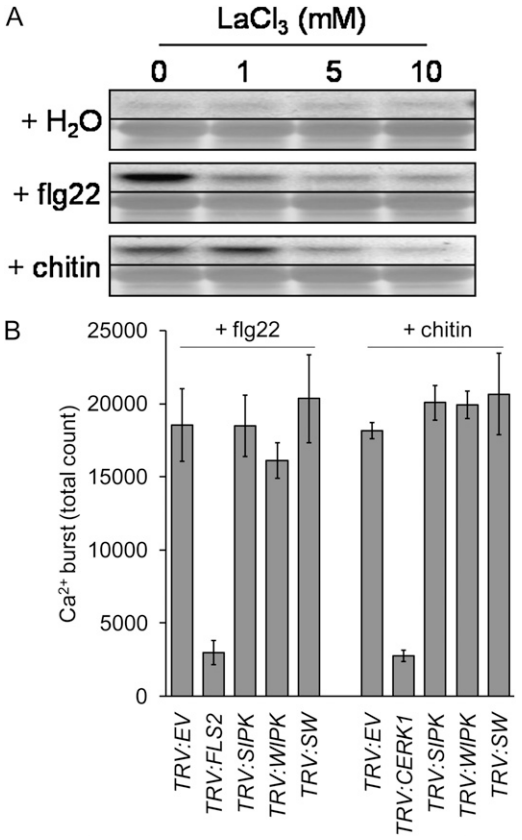

Figure 2. Apoplastic Ca^{2+} is required for the PAMP-triggered MAPK activation. A, The Ca^{2+} channel blocker $LaCl_3$ inhibits flg22- and chitin-induced MAPK activation. Proteins were extracted from leaf discs 15 min after treatment with flg22 or chitin together with increasing doses of $LaCl_3$. MAPK activation was monitored by western blot with anti-pTEpY antibody. Coomassie Brilliant Blue staining is shown to assess equal loading. B and C, Flg22-induced (B) and chitin-induced (C) Ca^{2+} bursts are not altered by VIGS of *NbSIPK* or *NbWIPK*. Ca^{2+} burst was measured in the *N. benthamiana* SLJR15 line silenced for the empty vector (*TRV*:*EV*), *NbFls2* (*TRV*:*FLS2*), *NbCerk1* (*TRV*:*CERK1*), *NbSIPK* (*TRV*:*SIPK*), *NbWIPK* (*TRV*:*WIPK*), or both (*TRV*:*SW*). Data are presented as average sums of photon counts during a 30-min measurement for 12 samples ± SD.

contrast, the response in *TRV*:*SIPK*, *TRV*:*WIPK*, and *TRV*:*SW* plants was indistinguishable from that observed in *TRV*:*EV* control plants. We observed comparable results after chitin treatment: the Ca^{2+} burst was compromised in *TRV*:*CERK1* plants but unchanged in leaves silenced for MAPKs relative to control plants (Fig. 2C). Thus, *NbSIPK* and *NbWIPK* are not required for the PAMP-induced Ca^{2+} burst.

PAMP perception leads to a defense-oriented transcriptional reprogramming of plant cells (Navarro et al., 2004; Zipfel et al., 2004, 2006). Using public microarray databases, we previously identified three marker genes that are rapidly and transiently upregulated upon PAMP treatment in *N. benthamiana*, namely *NbCYP71D20*, *NbACRE31*, and *NbACRE132* (Heese et al., 2007). To examine a role for Ca^{2+} influx in

flg22-induced gene expression, we monitored the transcription of these marker genes 1 h after elicitation with flg22 in the presence of increasing concentrations of $LaCl_3$ (Fig. 3) or EGTA (Supplemental Fig. S4B). *NbCYP71D20* expression was induced approximately 100-fold by flg22 compared with its accumulation in water-treated samples. This induction was reduced stepwise by increasing concentrations of $LaCl_3$ or EGTA and was approximately 20% of the untreated control in the presence of 10 mM $LaCl_3$ or EGTA. Similarly, the induction of *NbACRE31* and *NbACRE132* by flg22 treatment decreased by 90% and 95%, respectively, in samples cotreated with 10 mM $LaCl_3$ compared with untreated samples and decreased by 70% and 80%, respectively, in samples treated with 10 mM EGTA. This experiment shows that the apoplastic Ca^{2+} required for the PAMP-triggered Ca^{2+} burst is also necessary for the full induction of flg22-induced genes.

NbSIPK and *NbWIPK* Are Negative Regulators of the PAMP-Triggered ROS Burst

Since an increase of cytosolic Ca^{2+} is required for both the ROS burst (Fig. 1) and MAPK activation (Fig. 2), a direct linear pathway in which the Ca^{2+}-dependent ROS burst leads to MAPK activation is conceivable. Alternatively, it is also possible that Ca^{2+}-dependent MAPK activation triggers ROS production or that the pathways act independently downstream of the Ca^{2+} burst. To test whether the ROS burst is a prerequisite for MAPK activation, we assayed MAPK activation in the *TRV:RbohB* silenced plants, which are unable to produce ROS upon PAMP treatment (Fig. 4A). Fifteen minutes after flg22 or chitin elicitation, the anti-pTEpY signal observed in *TRV:RbohB* plants was similar to that observed in *TRV:EV* control plants. Thus, PAMP-induced MAPK activation occurred normally in the absence of the ROS burst. These results indicate that ROS production is not required for MAPK activation upon PAMP elicitation.

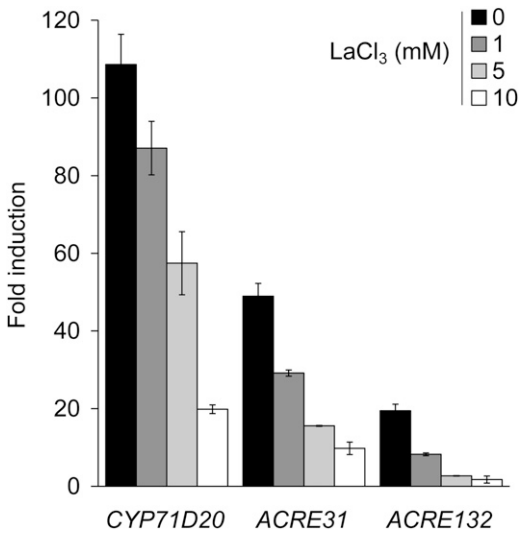

Figure 3. Apoplastic Ca^{2+} is required for flg22-induced gene expression. Increasing doses of $LaCl_3$ were added together with flg22. Induction of the marker genes *NbCYP71D20, NbACRE31,* and *NbACRE132* was monitored by qRT-PCR 60 min after treatment and normalized by *NbEF1α* gene expression. Data are presented as average fold induction compared with water-treated samples of three biological replicates ± SD.

We next tested the possibility of a direct linear pathway where Ca^{2+}-dependent MAPK activation leads to activation of the NADPH oxidase and ROS production. For this aim, we measured the ROS burst after PAMP treatment in *TRV:SIPK*, *TRV:WIPK*, or *TRV:SW* silenced plants. In *TRV:EV* control plants, flg22 triggered an initial ROS peak between 5 and 50 min following elicitation (Fig. 4B). The ROS production level returned to the basal state after 50 min, and a second broader peak of activity occurred 2 to 6 h after elicitation. This second burst was of lower amplitude compared with the first. In both *TRV:SIPK* and *TRV:WIPK* plants, the amplitude and duration of both ROS peaks were higher than in *TRV:EV* control plants. This effect was further enhanced in *TRV:SW* silenced plants, where the amplitude of the first and second peaks was 2 to 6 times higher than in *TRV:EV* plants. Interestingly, ROS production did not return to the basal level in *TRV:SW* silenced plants as observed in *TRV:EV* control plants, suggesting that the mechanism responsible for shutting down ROS production was absent or dysfunctional in these plants. The same trend was observed when the ROS burst was elicited with chitin, although on a lesser scale (Fig. 4C). Noteworthy, chitin induced only modest ROS production compared to flg22, consisting of a single sharp peak lasting 45 min. *TRV:WIPK* and *TRV:SW* silenced plants showed higher amplitude and duration of the chitin-induced ROS burst, whereas *TRV:NbSIPK* plants did not. To confirm these observations, we monitored the flg22- and chitin-induced ROS burst in Arabidopsis *mpk3* and *mpk6* single mutants (Supplemental Fig. S6). Interestingly, the ROS burst elicited by both flg22 and chitin was prolonged and enhanced in *mpk3* plants compared with wild-type ecotype Columbia plants. Only a slight increase of ROS production was observed in *mpk6* plants in response to chitin but not to flg22.

It was reported previously that *NbSIPK* and another closely related MAPK gene, *NbNTF6*, are required for induction of the *NbRbohB* gene upon pathogen attack (Asai et al., 2008). In addition, silencing of both kinase genes reduces the ROS accumulation after *Agrobacterium*-mediated transient expression of INF1 in *N. benthamiana* leaves (Asai et al., 2008). To test a potential role for *NbNTF6* in PAMP-induced ROS production, we generated VIGS constructs to silence *NbNTF6* (*TRV:NTF6*) or *NbSIPK* and *NbNTF6* together (*TRV:NS*). qRT-PCR analysis of the silenced plants showed that these constructs efficiently and specifically reduced the accumulation of *NbNTF6* transcripts (Supplemental Fig. S7). We assayed flg22- and chitin-triggered

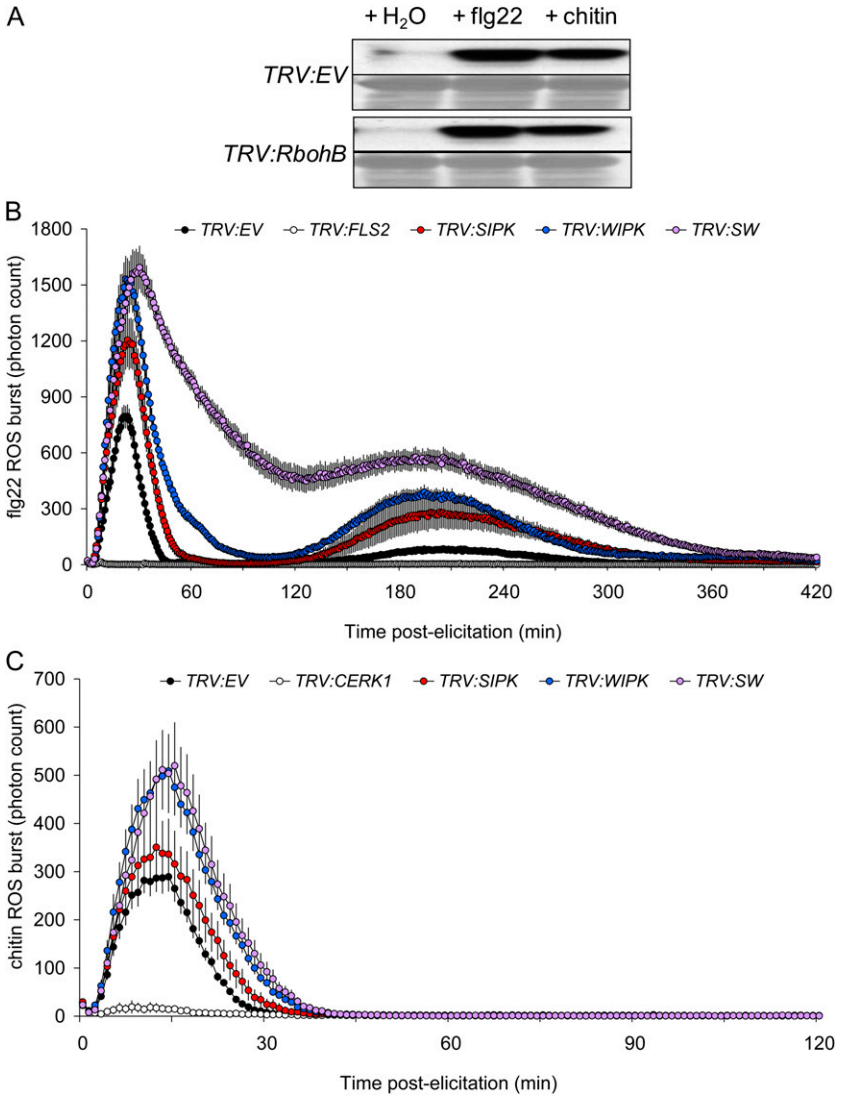

Figure 4. Silencing of *NbSIPK* and *NbWIPK* deregulates the PAMP-triggered ROS burst. A, MAPK activation is not altered by VIGS of *NbRbohB*. Proteins were extracted from leaf discs 15 min after treatment with flg22 or chitin. MAPK activation was monitored by western blot with anti-pTEpY antibody. Coomassie Brilliant Blue staining is shown to assess equal loading. B and C, Flg22-induced (B) and chitin-induced (C) ROS bursts are enhanced and last longer in plants silenced for *NbSIPK* and *NbWIPK*. No signal was detected after 45 min in chitin-treated plants. ROS burst was measured in the wild-type *N. benthamiana* line silenced for the empty vector (*TRV:EV*), *NbFls2* (*TRV:FLS2*), *NbCerk1* (*TRV:CERK1*), *NbSIPK* (*TRV:SIPK*), *NbWIPK* (*TRV:WIPK*), or both (*TRV:SW*). Data are presented as average signals of 12 samples ± SD.

ROS production in *TRV:SIPK*, *TRV:NTF6*, and *TRV:NS* silenced plants in comparison with control plants silenced for the empty vector or the individual PAMP receptor genes. As observed in Figure 4B and Supplemental Figure S7B, the flg22-induced ROS production was abolished in *TRV:FLS2* plants and slightly enhanced in *TRV:SIPK* plants compared with the *TRV:EV* control. However, the total ROS production in *TRV:NTF6* plants was similar to that observed in *TRV:EV* plants, and *TRV:NS* plants displayed the same enhancement of ROS production as observed in *TRV:SIPK* (Supplemental Fig. S7B). The same response pattern was observed when chitin was used for elicitation (Supplemental Fig. S7C). Therefore, *NbNTF6* is not involved in the activation of ROS production following flg22 or chitin elicitation in *N. benthamiana*. Altogether, these results indicate that the ROS burst and MAPK activation are initiated independently of each other after the PAMP-triggered transient increase of cytosolic Ca^{2+} concentration. Second, *NbSIPK* and especially *NbWIPK* seem to play roles in the negative regulation of ROS production after elicitation, whereas *NbNTF6* does not.

NbSIPK, But Not *NbWIPK*, Is Required for flg22-Induced Gene Expression

Elicitor recognition orchestrates extensive transcriptional reprogramming of the affected cell that is critical for plant immunity (Navarro et al., 2004; Zipfel et al., 2004, 2006). To examine roles for MAPKs and the ROS burst in transcriptional reprogramming, we monitored the expression of *NbCYP71D20*, *NbACRE31*, and *NbACRE132* following flg22 treatment in *N. benthamiana* plants compromised for the ROS burst or MAPK expression. Additional controls were plants silenced for PAMP receptors or the empty vector. As expected, VIGS of *NbFls2* severely compromised the induction of the three marker genes upon flg22 elicitation (Fig. 5). Importantly, VIGS leads to incomplete knockdown of

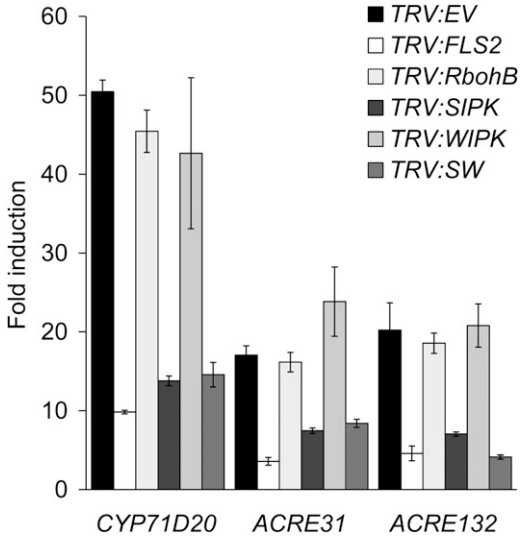

Figure 5. *NbSIPK* is required for flg22-induced gene expression. Total RNA was extracted from *N. benthamiana* wild-type plants silenced for the empty vector (*TRV*:*EV*), *NbFls2* (*TRV*:*FLS2*), *NbRbohB* (*TRV*:*RbohB*), *NbSIPK* (*TRV*:*SIPK*), *NbWIPK* (*TRV*:*WIPK*), or both (*TRV*:*SW*). Induction of the marker genes *NbCYP71D20*, *NbACRE31*, and *NbACRE132* was monitored by qRT-PCR 60 min after treatment and normalized by *NbEF1α* gene expression. Data are presented as average fold induction compared with water-treated samples of three biological replicates ± SD.

the targeted gene, which explains the remaining transcript accumulation (approximately 20% of empty vector induction). A similar loss of induction (approximately 50%–70%) of the three defense genes was observed in *TRV*:*SIPK* and *TRV*:*SW* plants. Strikingly, in *TRV*:*WIPK* and *TRV*:*RbohB* plants, we observed the same level of gene induction as in *TRV*:*EV* control plants. This suggests that neither *NbWIPK* nor *NbRbohB* is required for flg22-induced gene expression in *N. benthamiana*. Thus, NbSIPK contributes strongly to the induction of PAMP-induced genes, and NbSIPK and NbWIPK act nonredundantly in this response.

Both *NbSIPK* and *NbWIPK* Are Required for Bacterial Immunity

The ultimate outcome of PTI is the mounting of efficient defense responses that restrict pathogen growth (Zipfel et al., 2004). To test roles for early signaling events in bacterial immunity, we assessed the growth of virulent and nonpathogenic strains of *Pseudomonas syringae* in plants impaired for ROS production or MAPK activation. *P. syringae* pv *tabaci* 11528 (*Pta* 11528) causes wildfire disease on soybean (*Glycine max*) and tobacco plants (Gasson, 1980). One *hypersensitive response and pathogenicity* (*hrp*) mutant of this strain (*Pta* 11528 *hrcV*$^-$) has lost the ability to inject type III effectors into the host cell and therefore is nonpathogenic (Oh and Collmer, 2005). We spray inoculated silenced plants with bacterial suspensions as an effective method to study PTI (Zipfel et al., 2004). In *TRV*:*EV* control plants, the virulent strain *Pta* 11528 grew 1,000-fold more than the nonpathogenic strain *Pta* 11528 *hrcV*$^-$ (Fig. 6A). In *TRV*:*FLS2* and *TRV*:*CERK1* plants, both strains grew approximately 10-fold more than in control plants, demonstrating the contribution of these receptors to the defense response. In *TRV*:*RbohB* silenced plants, no growth difference

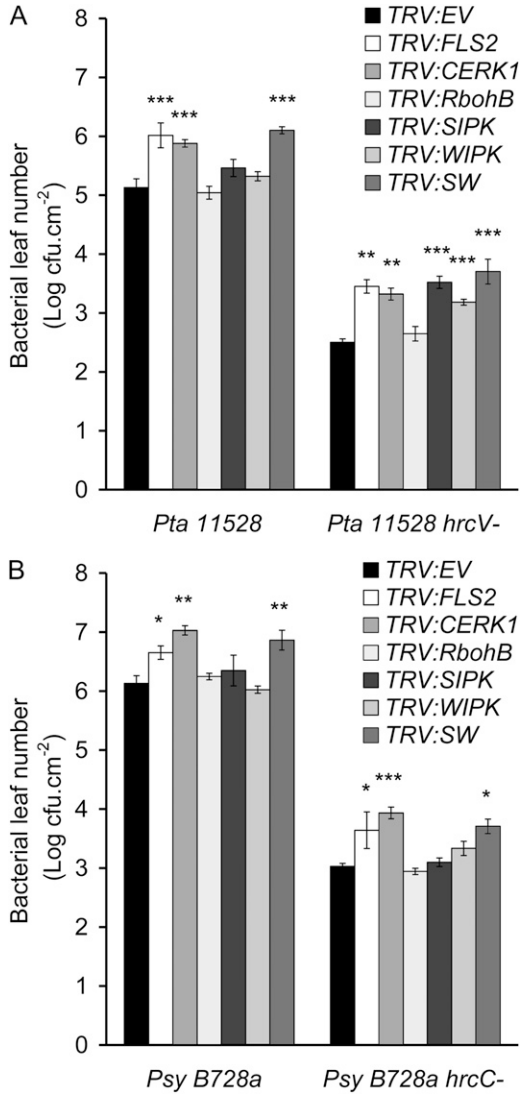

Figure 6. *NbSIPK* and *NbWIPK* but not *NbRbohB* are required for bacterial immunity. A, Virulent *Pta* 11528 and nonpathogenic *hrcV*$^-$ mutant strains grow more on plants silenced for *NbSIPK* and *NbWIPK*. B, Virulent *Psy* B728a and nonpathogenic *hrcC*$^-$ mutant strains grow more on plants silenced for *NbSIPK* and *NbWIPK*. Bacteria were spray inoculated on *N. benthamiana* wild-type plants silenced for the empty vector (*TRV*:*EV*), *NbFls2* (*TRV*:*FLS2*), *NbCerk1* (*TRV*:*CERK1*), *NbRbohB* (*TRV*:*RbohB*), *NbSIPK* (*TRV*:*SIPK*), *NbWIPK* (*TRV*:*WIPK*), or both (*TRV*:*SW*). Bacterial counts were performed 2 d after inoculation. Statistical significance was assessed by comparison with *TRV*:*EV* using one-way ANOVA followed by Dunnett's test. * $P < 0.1$, ** $P < 0.05$, *** $P < 0.01$. cfu, Colony-forming units.

compared with *TRV*:*EV* plants could be observed, suggesting that the contribution of the ROS burst to restriction of pathogen growth is negligible in this system. In contrast, growth of virulent *Pta* 11528 was similar in *TRV*:*SW* plants to that observed in *TRV*:*FLS2* and *TRV*:*CERK1* plants, almost 10-fold more than in control plants. In addition, the nonpathogenic strain *Pta* 11528 *hrcV*$^-$ also grew more on *TRV*:*SIPK*, *TRV*:*WIPK*, and *TRV*:*SW* silenced plants. This experiment shows that the MAPKs NbSIPK and NbWIPK are required for full bacterial immunity.

To extend these results, we assayed the growth of another virulent bacterial strain adapted to *N. benthamiana*, *P. syringae* pv *syringae* B728a (*Psy* B728a; Vinatzer et al., 2006) and its nonpathogenic *hrp* mutant (*Psy* B728a *hrcC*$^-$; Mohr et al., 2008). Two days after spray inoculation, *Psy* B728a grew 1,000-fold more than the *hrp* mutant on *TRV*:*EV* plants (Fig. 6B). For both strains, the absence of individual PAMP receptors in *TRV*:*FLS2* and *TRV*:*CERK1* silenced plants resulted in a 5 to 10 times enhancement of growth compared with that on the *TRV*:*EV* control plants. The bacterial counts in *TRV*:*RbohB* plants were similar to those in control plants. Finally, silencing of *NbSIPK* and *NbWIPK* together in *TRV*:*SW* plants led to a significant growth enhancement for both strains. Taken together, these results indicate that both NbSIPK and NbWIPK make important contributions to PTI in *N. benthamiana*.

DISCUSSION

The data presented in this work demonstrate the role and hierarchy of key signaling events during PTI. Most of the known early signaling events associated with PTI can be measured in *N. benthamiana*, notably the induction of ROS production, MAPK activation, and transcriptional reprogramming (Hann and Rathjen, 2007; Nguyen et al., 2010). We further created a stable transgenic line expressing the Ca^{2+} reporter Aequorin to allow in vivo measurement of the rapid transient rise of cytosolic Ca^{2+} following PAMP treatment. We used a pharmacological approach to study the role of Ca^{2+} during signaling because no genetic data concerning Ca^{2+} channels exist. We could suppress the Ca^{2+} influx completely with inhibitors of apoplastic Ca^{2+} release. We also showed that *NbRbohB* silencing completely abrogated the ROS burst in response to PAMPs. NbRbohB is the ortholog of AtRbohD in Arabidopsis, which has been shown to be responsible for the ROS production induced by flg22 (Nühse et al., 2007; Zhang et al., 2007). We show that the major MAPKs activated in response to PAMP in *N. benthamiana* are indeed NbSIPK and NbWIPK and that the corresponding genes act nonredundantly in PTI. The kinetics of the different responses presented here are in accordance with a hierarchal series of events and a bifurcated signaling pathway that we demonstrated by using a combined approach of VIGS and pharmacological inhibitors.

An influx of Ca^{2+} from external stores was critical for the activation of all tested responses downstream of PAMP perception. Using the transgenic *N. benthamiana* SLJR15 line expressing Aequorin, we found that treatment of leaves with flg22 or chitin induced a rapid Ca^{2+} burst, but with differences in the profiles induced by these two elicitors. This accords with previous studies in tobacco and Arabidopsis (Lecourieux et al., 2005; Aslam et al., 2009). One interpretation of this result is that different Ca^{2+} signatures could encode a degree of specificity for subsequent signaling events (Hetherington and Brownlee, 2004; Dodd et al., 2010). However, the same hierarchy of downstream signaling events was observed with both PAMPs. Our data do not shed light on this; nevertheless, the different Ca^{2+} responses to flg22 and chitin seen here were correlated with the massive difference in the amplitude of ROS production triggered by the two different PAMPs.

Challenge of *N. benthamiana* leaves with flg22 or chitin rapidly activated two MAPKs. We confirmed through gene silencing that the two most prominent MAPK species activated are NbSIPK and NbWIPK and that their activation is at least partially Ca^{2+} dependent but ROS independent. Although both SIPK and WIPK are often activated together by various stresses and are likely the targets of a common upstream MAPK kinase, these two terminal kinases appear to play somewhat different but intertwined biological roles (Kim and Zhang, 2004). NbWIPK plays a more prominent role than NbSIPK in the negative regulation of the ROS burst triggered by PAMP application. On the other hand, NbSIPK alone was required for full induction of flg22-regulated genes, which is in accordance with previous studies on the *mpk6* mutant of Arabidopsis or the *SIPK*-silenced tobacco line (Menke et al., 2004; Samuel et al., 2005). MAPK pathways control WRKY transcription factor activity, providing a partial explanation for transcriptional reprogramming upon PAMP elicitation (Asai et al., 2002; Miao et al., 2007). We found that both *NbSIPK* and *NbWIPK* were necessary for bacterial immunity in *N. benthamiana*. We were able to measure significant growth enhancements of both virulent and nonpathogenic strains on silenced plants. NbSIPK and NbWIPK appear to act nonredundantly because of their differential requirement for defense gene induction and the additive effects of their silencing on bacterial growth. As only *NbSIPK* is required for full induction of PAMP-responsive genes, it is likely that the transcriptional reprogramming alone does not convey all the signal leading to bacterial immunity; this latter could be strengthened by metabolic changes directly regulated by one or both MAPKs. We note that *NbSIPK* and *NbWIPK* are also required for effector-triggered immunity against the avirulent bacterial strain *Pseudomonas cichorii* (Sharma et al., 2003). Thus, these kinases play multiple essential roles in antibacterial immunity. We cannot exclude the possibility that other MAPKs, close *NbSIPK* or *NbWIPK* homologs such as *NbNTF4* (Ren et al., 2006) or *NbNTF6* (Asai et al., 2008), were

also activated by PAMP treatment but not clearly detected by the anti-pTEpY antibody.

Activation of MAPKs was partially dependent on the Ca^{2+} influx. Increasing amounts of both $LaCl_3$ and EGTA led progressively to strong inhibition of the appearance of activated MAPK forms. Similar results have been described in a number of different systems (Lebrun-Garcia et al., 1998; Fellbrich et al., 2000; Lee et al., 2001). A very recent paper found that MAPK activation in Arabidopsis is only partially dependent on Ca^{2+} (Boudsocq et al., 2010). As MAPK activation is thought to be a very early event in PTI signaling, it seems likely that the Ca^{2+} influx is one of the first events after receptor stimulation. CDPKs regulate fungal elicitor signaling in tobacco and the FLS2 pathway in Arabidopsis (Kobayashi et al., 2007; Boudsocq et al., 2010). Cross talk between MAPK and CDPK pathways has been described, but also, one or the other class of protein kinases may be more important depending on the stimuli perceived (Ludwig et al., 2005).

Production of ROS directed by PAMP treatment was strictly dependent on Ca^{2+} influx. Similar results have been described in tobacco cells using pharmacological inhibitors after cryptogein treatment (Pugin et al., 1997). In our experiments, inhibition of the ROS burst occurred at lower inhibitor concentrations than for MAPK inhibition. One possibility is that Ca^{2+} is required at more than one point in the ROS pathway. The presence of Ca^{2+}-binding EF hands in the N-terminal regulatory tail of the Rboh enzyme is consistent with this idea (Ogasawara et al., 2008). In addition, it was shown recently that members of the CDPK family can activate Rboh enzymes through phosphorylation of their N-terminal extension (Kobayashi et al., 2007). Thus, Ca^{2+} may be required immediately post stimulation of the PAMP receptor and again at activation of the Rboh enzyme. Despite this complexity, our data show that ROS production and MAPK activation lie on different pathways, because silencing of the major active MAPK isoforms did not disrupt ROS production.

At present, the relationships between MAPK and ROS production downstream of PAMP perception are contradictory. Earlier studies in transgenic tobacco expressing the plasma membrane receptor Cf9 have shown that, upon perception of the fungal effector Avr9, MAPK activation and ROS production are independent signaling events that both require calcium influx (Romeis et al., 1999). However, both Arabidopsis MPK6 and its ortholog tobacco SIPK can be activated by hydrogen peroxide supplied exogenously (Samuel et al., 2000; Yuasa et al., 2001). In contrast, Zhang et al. (2007) showed that expression of a constitutive gain-of-function form of AtMKK5 ($AtMKK5^{DD}$) in Arabidopsis led to activation of MPK6 and MPK3 in the absence of elicitation and to a further defense response, callose deposition into cell walls. As these authors also observed a reduction of callose deposition upon flg22 treatment in an *AtrbohD* mutant, their results suggest indirectly that MAPK activation led to ROS production and then to callose deposition in Arabidopsis. Moreover, this study shows that the *P. syringae* effector HopAI1-1 is able to suppress MAPK activation through its phospho-Thr lyase activity and that expression of HopAI1-1 in transgenic Arabidopsis plants also inhibits flg22-induced ROS production, therefore positioning MAPK activation upstream of ROS production in this pathway (Zhang et al., 2007). Nonetheless, a direct link between these two responses could not be evidenced, as alternative targets for HopAI1-1, which could be required for RbohD activation, cannot be ruled out. Arabidopsis lines lacking both MPK3 and MPK6 are sickly and unsuitable for PTI studies (Wang et al., 2007, 2008). This prevents a direct study of the role of both MAPKs in ROS production. However, our data are unequivocal and place these events in different pathways. Finally, Asai et al. (2008) showed that *NbSIPK* and *NbNTF6* were both required for the induction of *NbRbohB* during pathogen attack and that silencing of both kinase genes reduces ROS accumulation 2 d after *Agrobacterium*-mediated transient expression of INF1 inside *N. benthamiana* cells. Here, we saw the rapid and transient ROS production triggered by purified PAMPs in plants impaired for MAPK activation, and conversely, we detected MAPK activation in plants impaired for ROS production. Our data indicate clearly that MAPK activation and ROS production occur independently of each other but that both lie downstream of the transient cytosolic Ca^{2+}.

We found that the amplitude and duration of the PAMP-induced Ca^{2+} burst were increased in the absence of the ROS burst. A number of studies show the existence of ROS-gated calcium channels, notably in the plasma membrane of guard cells (Mori and Schroeder, 2004). However, no negative regulatory role for ROS in these channels has been described. It is possible that ROS shut down permeable channels at the plasma membrane that mediate Ca^{2+} influx. Alternatively, ROS could positively regulate the Ca^{2+}-ATPase pump that removes Ca^{2+} from the cytosol, thus preventing reversal of the transient increase in cytosolic Ca^{2+} concentration. It is interesting that calmodulin, a small ubiquitous Ca^{2+}-binding protein, plays a crucial role in the regulation of Ca^{2+} signaling by activating Ca^{2+}-ATPase pumps (Malmström et al., 1997; Harper et al., 1998; Chung et al., 2000) but can also inhibit Ca^{2+} channels of the CNGC family (Arazi et al., 2000). A recent study showed that hydrogen peroxide enhances calmodulin expression very rapidly (Hu et al., 2007), which could enhance the Ca^{2+}-pump activity and reduce the concentration of Ca^{2+} within the cell. This provides a possible mechanism to explain the increased cytoplasmic Ca^{2+} levels in the absence of ROS production after PAMP elicitation.

We also found that amplitude and particularly duration of the ROS burst were dramatically increased in the absence of MAPK activation. This unexpected result is consistent with a previous report of massive

ROS accumulation after harpin treatment of a stable transgenic tobacco line silenced for SIPK expression (Samuel et al., 2005). A central function of SIPK in the cell, therefore, may be to monitor and regulate the cellular redox status (Samuel et al., 2005). On the other hand, it has been suggested that *NbRbohB* is under the transcriptional control of *NbSIPK* and *NbNTF6* (Asai et al., 2008). However, in this study, the accumulation of *NbRbohB* transcripts in plants silenced for *NbSIPK* and *NbWIPK*, or *NbNTF6* and *NbSIPK*, was less than 2-fold that in the control plants (data not shown). An effect on *NbRbohB* expression seems unlikely, because the first ROS burst started less than 5 min after elicitation, which would presumably allow insufficient time for de novo transcription and translation of the Rboh enzyme. Finally, in chitin experiments, *NbWIPK* but not *NbSIPK* played an important role in shutting down ROS production. We made similar observations in the Arabidopsis *mpk3* mutant in response to flg22 or chitin. Rboh enzymes are regulated synergistically by phosphorylation and Ca^{2+} binding in the N-terminal cytosolic region (Ogasawara et al., 2008); here, we found that their activation was independent of *NbSIPK* and *NbWIPK*, but these enzymes, in particular NbWIPK, may yet play a role in Rboh inactivation, perhaps via the numerous phospho sites in the N-terminal extension (Benschop et al., 2007; Nühse et al., 2007) or by indirect activation of phosphatases. The negative feedbacks exerted by ROS on Ca^{2+} influx and by MAPKs on ROS production are a potential means of fine-tuning PTI signaling once it has been established, preventing prolonged activation of the signal that could cause cellular damage. Negative control of signaling is essential for appropriately timed, quantified, and coordinated responses to a specific stimulus, whereas the positive elements are essential to initiate signal transduction (Bowler and Chua, 1994).

To summarize, our analyses using whole *N. benthamiana* plants as a versatile study model for PTI provide important evidence for the role of early signaling events in establishing immunity against bacterial pathogens and highlight the relationships between long known components of the signaling cascade downstream of PAMP perception. The immediate challenge highlighted by this work is to discover how the transient increase in cytoplasmic Ca^{2+} is interpreted by the cell into a functional immune response.

MATERIALS AND METHODS

All the experiments in this study were independently performed at least three times with similar results. One representative set of data is shown, unless otherwise stated.

Plant Material

Nicotiana benthamiana plants were grown in a controlled-environment chamber under 16 h of light. The transgenic line SLJR15 expressing Aequorin (Knight et al., 1993) was created by leaf disc *Agrobacterium tumefaciens*-mediated transformation and regeneration of callus. Primary transformants were selected on kanamycin (50 μg mL^{-1}). A single insertion line was further screened by selection of the T2 plants on kanamycin and subsequent selfing.

Arabidopsis (*Arabidopsis thaliana*) ecotype Columbia, *fls2* (Heese et al., 2007), *cerk1-2* (Miya et al., 2007), *mpk3* (SALK_151594), and *mpk6* (SALK_127507) plants were grown in a controlled-environment chamber under 8 h of light for 5 weeks.

Chemicals

All the chemicals used in this study were purchased from Sigma unless otherwise stated.

VIGS in *N. benthamiana*

VIGS was performed using a TRV vector as described (Liu et al., 2002; Peart et al., 2002). Three weeks after inoculation, silenced leaves were used for subsequent studies. The following primers adapted from Yoshioka et al. (2003) and Asai et al. (2008) were used for *Eco*RI cloning into pYL156; the *Eco*RI restriction site is indicated as lowercase: for *NbRbohB*, 5′-ccgaattcAATCATCATCCGCACCACCATCAC-3′ and 5′-ccgaattcACGCATCATCATTGGACTTGCCGC-3′; for *NbSIPK*, 5′-ccgaattcTTCTACACAGGGACTTGAAGC-3′ and 5′-ccgaattcTGATCTCTACCAGGAAATAGG-3′; for *NbWIPK*, 5′-ccgaattcGTTACGAAGGGAGTTTTCTGA-3′ and 5′-ccgaattcTCCGTCATATTCTCGTTCTCT-3′; and for *NbNTF6*, 5′-ccggaattcCGCTAGAACCACTTCAGAG-3′ and 5′-ccgaattcTAGAGCCTCGTTCCATATGAGC-3′.

ROS Assay

Detection of ROS production was monitored by a luminol-based assay on leaf disc samples (Keppler et al., 1989). Leaf discs dispatched on a 96-well plate were incubated overnight in water. Before measurement, the water was removed and 100 μL of assay solution (17 mM luminol, 1 μM horseradish peroxidase, and 100 nM flg22 [Peptron] or 100 μg mL^{-1} chitin) was added to the wells. Luminescence was measured using a Photek camera system and acquired over time.

Calcium Assay

Transient increase of cytosolic Ca^{2+} concentration was monitored in the *N. benthamiana* SLJR15 transgenic line. Leaf discs dispatched on a 96-well plate were incubated overnight in 12.5 μM coelenterazin (LUX Innovate). Before measurement, the solution was removed and 100 μL of assay solution (100 nM flg22 or 100 μg mL^{-1} chitin) was added to the wells. Luminescence was measured using a Photek camera system and acquired over time.

qRT-PCR

Total RNA were isolated from leaf disc samples with the TRI reagent (Invitrogen) following the manufacturer's instructions. Total RNA were quantified with a Nanodrop spectrophotometer (Roche). Synthesis of the first strand of cDNA was performed on 3 μg of RNA by RT with the SuperScript II kit from Invitrogen following the manufacturer's instructions. qPCR were performed with SYBR Green in triplicate with a PTC-200 Peltier Thermal Cycler (MJ Research), and the data were collected and analyzed with the Chromo 4 Continuous Fluorescence detection system. The *NbEF1α* transcript was analyzed as an internal control and used to normalize the values for transcript abundance. The following primers were used for amplification: for *NbRbohB*, 5′-TTTCTCTGAGGTTTGCCAGCCACCACCTAA-3′ and 5′-GCCTTCATGTTGTTGACAATGTCTTTAACA-3′; for *NbSIPK*, 5′-ACGAGCCCATTTGCATGACTCCC-3′ and 5′-AGCTCCTTCATCTGTTCCTCCGT-3′; for *NbWIPK*, 5′-CCGATCTGCCCCGTTCCATCC-3′ and 5′-TCAGGATTCAGCGACAAAGCTTCC-3′; for *NbNTF6*, 5′-AAGGGGTTCCAACACATGAGGGG-3′ and 5′-GCCACGGCCGACAGGTTGAA-3′; for *NbCYP71D20*, 5′-AAGGTCCACCGCACCATGTCCTTAGAG-3′ and 5′-AAGAATTCCTTGCCCCTTGAGTACTTGC-3′; for *NbACRE31*, 5′-AAGGTCCCGTCTTCGTCGGATCTTCG-3′ and 5′-AAGAATTCGGCCATCGTGATCTTGGTC-3′; for *NbACRE132*, 5′-AAGGTCCAGCGAAGTCTCTGAGGGTGA-3′ and 5′-AAGAATTCCAATCCTAGCTCTGGCTCCTG-3′; and for *NbEF1α*, 5′-AAGGTCCAGTATGCCTGGGTGCTTGAC-3′ and 5′-AAGAATTCACAGGGACAGTTCCAATACCAC-3′.

MAPK Activation Assay

The anti-pTEpY antibody was purchased from Cell Signaling (NEB 4370S) and used following the manufacturer's instructions. Total proteins were extracted in Lacus buffer (50 mM Tris-HCl, pH 7.5, 10 mM $MgCl_2$, 15 mM EGTA, 100 mM NaCl, 2 mM dithiothreitol, 1 mM NaF, 1 mM NaMo, 0.5 mM $NaVO_3$, 30 mM β-glycerophosphate, and 0.1% Nonidet P-40) supplemented with 100 nM calyculin A, 0.5 mM phenylmethylsulfonyl fluoride, and 1% anti-protease cocktail (P9599; Sigma) and were quantified with the Bradford assay. Forty micrograms of proteins was loaded per lane for the western blots.

Bacterial Growth Assay

Pseudomonas syringae pv *tabaci* 11528 (and *hrcV*$^-$) and *P. syringae* pv *syringae* B728a (and *hrcC*$^-$) were streaked from glycerol stocks to single colonies on King's B medium supplemented with adequate antibiotics (100 μg mL^{-1} rifampicin, 50 μg mL^{-1} kanamycin, and 50 μg mL^{-1} spectinomycin). Bacteria were then cultured in liquid L medium until optical density at 600 nm (OD_{600}) reached 0.6, harvested by centrifugation, and resuspended in 10 mM $MgCl_2$ to OD_{600} = 0.02 for the virulent strains and OD_{600} = 0.2 for the nonpathogenic strains. Silwett L-77 (0.04%) was added to the bacterial suspension just before spraying. Sprayed plants were kept in high humidity under a plastic dome until leaf disc samples were harvested, 2 d after inoculation. Samples (0.38 cm^2) were ground and subsequently serial diluted in 10 mM $MgCl_2$ before plating on King's B medium supplemented with adequate antibiotics. Bacterial colonies were counted after 48 h of incubation at 28°C.

Supplemental Data

The following materials are available in the online version of this article.

Supplemental Figure S1. The Ca^{2+} chelator EGTA and the Ca^{2+} channel blocker $LaCl_3$ suppress PAMP-triggered Ca^{2+} burst.

Supplemental Figure S2. *NbRbohB* is responsible for the PAMP-triggered ROS burst.

Supplemental Figure S3. Kinetics of MAPK activation following PAMP elicitation.

Supplemental Figure S4. The Ca^{2+} chelator EGTA inhibits PAMP-induced MAPK activation and gene expression.

Supplemental Figure S5. NbSIPK and NbWIPK are activated by PAMPs.

Supplemental Figure S6. The PAMP-triggered ROS burst is enhanced and prolonged in the Arabidopsis *mpk3* mutant.

Supplemental Figure S7. *NbNTF6* is not involved in the PAMP-triggered ROS burst.

ACKNOWLEDGMENTS

We are grateful to Allan Collmer, Boris Vinatzer, and Scott Peck for the gifts of *Pta* 11528 *hrcV*$^-$, *Psy* B728a *hrcC*$^-$, and *mpk3* and *mpk6* mutants, respectively. We thank Alexi Balmuth and Matthew Smoker for developing the *N. benthamiana* Aequorin transgenic line. J.P.R. is a Future Fellow of the Australian Research Council (FT0992129).

Received December 22, 2010; accepted March 28, 2011; published April 8, 2011.

LITERATURE CITED

Ali R, Ma W, Lemtiri-Chlieh F, Tsaltas D, Leng Q, von Bodman S, Berkowitz GA (2007) Death don't have no mercy and neither does calcium: *Arabidopsis* CYCLIC NUCLEOTIDE GATED CHANNEL2 and innate immunity. Plant Cell **19:** 1081–1095

Arazi T, Kaplan B, Fromm H (2000) A high-affinity calmodulin-binding site in a tobacco plasma-membrane channel protein coincides with a characteristic element of cyclic nucleotide-binding domains. Plant Mol Biol **42:** 591–601

Asai S, Ohta K, Yoshioka H (2008) MAPK signaling regulates nitric oxide and NADPH oxidase-dependent oxidative bursts in *Nicotiana benthamiana*. Plant Cell **20:** 1390–1406

Asai T, Tena G, Plotnikova J, Willmann MR, Chiu WL, Gomez-Gomez L, Boller T, Ausubel FM, Sheen J (2002) MAP kinase signalling cascade in Arabidopsis innate immunity. Nature **415:** 977–983

Aslam SN, Erbs G, Morrissey KL, Newman MA, Chinchilla D, Boller T, Molinaro A, Jackson RW, Cooper RM (2009) Microbe-associated molecular pattern (MAMP) signatures, synergy, size and charge: influences on perception or mobility and host defence responses. Mol Plant Pathol **10:** 375–387

Benschop JJ, Mohammed S, O'Flaherty M, Heck AJ, Slijper M, Menke FL (2007) Quantitative phosphoproteomics of early elicitor signaling in Arabidopsis. Mol Cell Proteomics **6:** 1198–1214

Blume B, Nürnberger T, Nass N, Scheel D (2000) Receptor-mediated increase in cytoplasmic free calcium required for activation of pathogen defense in parsley. Plant Cell **12:** 1425–1440

Boller T, Felix G (2009) A renaissance of elicitors: perception of microbe-associated molecular patterns and danger signals by pattern-recognition receptors. Annu Rev Plant Biol **60:** 379–406

Boudsocq M, Willmann MR, McCormack M, Lee H, Shan L, He P, Bush J, Cheng SH, Sheen J (2010) Differential innate immune signalling via Ca (2+) sensor protein kinases. Nature **464:** 418–422

Boutrot F, Segonzac C, Chang KN, Qiao H, Ecker JR, Zipfel C, Rathjen JP (2010) Direct transcriptional control of the Arabidopsis immune receptor FLS2 by the ethylene-dependent transcription factors EIN3 and EIL1. Proc Natl Acad Sci USA **107:** 14502–14507

Bowler C, Chua NH (1994) Emerging themes of plant signal transduction. Plant Cell **6:** 1529–1541

Chinchilla D, Bauer Z, Regenass M, Boller T, Felix G (2006) The *Arabidopsis* receptor kinase FLS2 binds flg22 and determines the specificity of flagellin perception. Plant Cell **18:** 465–476

Chinchilla D, Zipfel C, Robatzek S, Kemmerling B, Nürnberger T, Jones JD, Felix G, Boller T (2007) A flagellin-induced complex of the receptor FLS2 and BAK1 initiates plant defence. Nature **448:** 497–500

Chung WS, Lee SH, Kim JC, Heo WD, Kim MC, Park CY, Park HC, Lim CO, Kim WB, Harper JF, et al (2000) Identification of a calmodulin-regulated soybean Ca^{2+}-ATPase (SCA1) that is located in the plasma membrane. Plant Cell **12:** 1393–1407

Dahan J, Pichereaux C, Rossignol M, Blanc S, Wendehenne D, Pugin A, Bourque S (2009) Activation of a nuclear-localized SIPK in tobacco cells challenged by cryptogein, an elicitor of plant defence reactions. Biochem J **418:** 191–200

Dodd AN, Kudla J, Sanders D (2010) The language of calcium signaling. Annu Rev Plant Biol **61:** 593–620

Fellbrich G, Blume B, Brunner F, Hirt H, Kroj T, Ligterink W, Romanski A, Nürnberger T (2000) *Phytophthora parasitica* elicitor-induced reactions in cells of *Petroselinum crispum*. Plant Cell Physiol **41:** 692–701

Garcia-Brugger A, Lamotte O, Vandelle E, Bourque S, Lecourieux D, Poinssot B, Wendehenne D, Pugin A (2006) Early signaling events induced by elicitors of plant defenses. Mol Plant Microbe Interact **19:** 711–724

Gasson MJ (1980) Indicator technique for antimetabolic toxin production by phytopathogenic species of *Pseudomonas*. Appl Environ Microbiol **39:** 25–29

Gimenez-Ibanez S, Hann DR, Ntoukakis V, Petutschnig E, Lipka V, Rathjen JP (2009) AvrPtoB targets the LysM receptor kinase CERK1 to promote bacterial virulence on plants. Curr Biol **19:** 423–429

Gómez-Gómez L, Boller T (2000) FLS2: an LRR receptor-like kinase involved in the perception of the bacterial elicitor flagellin in Arabidopsis. Mol Cell **5:** 1003–1011

Goodin MM, Zaitlin D, Naidu RA, Lommel SA (2008) *Nicotiana benthamiana*: its history and future as a model for plant-pathogen interactions. Mol Plant Microbe Interact **21:** 1015–1026

Hann DR, Rathjen JP (2007) Early events in the pathogenicity of *Pseudomonas syringae* on *Nicotiana benthamiana*. Plant J **49:** 607–618

Harper JF, Hong B, Hwang I, Guo HQ, Stoddard R, Huang JF, Palmgren MG, Sze H (1998) A novel calmodulin-regulated Ca^{2+}-ATPase (ACA2) from Arabidopsis with an N-terminal autoinhibitory domain. J Biol Chem **273:** 1099–1106

Heese A, Hann DR, Gimenez-Ibanez S, Jones AM, He K, Li J, Schroeder JI, Peck SC, Rathjen JP (2007) The receptor-like kinase SERK3/BAK1 is

a central regulator of innate immunity in plants. Proc Natl Acad Sci USA **104:** 12217–12222

Hetherington AM, Brownlee C (2004) The generation of Ca(2+) signals in plants. Annu Rev Plant Biol **55:** 401–427

Hu X, Jiang M, Zhang J, Zhang A, Lin F, Tan M (2007) Calcium-calmodulin is required for abscisic acid-induced antioxidant defense and functions both upstream and downstream of H_2O_2 production in leaves of maize (*Zea mays*) plants. New Phytol **173:** 27–38

Iizasa E, Mitsutomi M, Nagano Y (2010) Direct binding of a plant LysM receptor-like kinase, LysM RLK1/CERK1, to chitin in vitro. J Biol Chem **285:** 2996–3004

Jeworutzki E, Roelfsema MR, Anschütz U, Krol E, Elzenga JT, Felix G, Boller T, Hedrich R, Becker D (2010) Early signaling through the Arabidopsis pattern recognition receptors FLS2 and EFR involves Ca-associated opening of plasma membrane anion channels. Plant J **62:** 367–378

Jones JD, Dangl JL (2006) The plant immune system. Nature **444:** 323–329

Kadota Y, Furuichi T, Ogasawara Y, Goh T, Higashi K, Muto S, Kuchitsu K (2004) Identification of putative voltage-dependent Ca^{2+}-permeable channels involved in cryptogein-induced Ca^{2+} transients and defense responses in tobacco BY-2 cells. Biochem Biophys Res Commun **317:** 823–830

Keppler LD, Atkinson MM, Baker CJ (1989) Active oxygen production during a bacteria-induced hypersensitive reaction in tobacco suspension cells. Phytopathology **79:** 974–978

Kim CY, Zhang S (2004) Activation of a mitogen-activated protein kinase cascade induces WRKY family of transcription factors and defense genes in tobacco. Plant J **38:** 142–151

Knight MR, Read ND, Campbell AK, Trewavas AJ (1993) Imaging calcium dynamics in living plants using semi-synthetic recombinant aequorins. J Cell Biol **121:** 83–90

Kobayashi M, Ohura I, Kawakita K, Yokota N, Fujiwara M, Shimamoto K, Doke N, Yoshioka H (2007) Calcium-dependent protein kinases regulate the production of reactive oxygen species by potato NADPH oxidase. Plant Cell **19:** 1065–1080

Kunze G, Zipfel C, Robatzek S, Niehaus K, Boller T, Felix G (2004) The N terminus of bacterial elongation factor Tu elicits innate immunity in *Arabidopsis* plants. Plant Cell **16:** 3496–3507

Lebrun-Garcia A, Ouaked F, Chiltz A, Pugin A (1998) Activation of MAPK homologues by elicitors in tobacco cells. Plant J **15:** 773–781

Lecourieux D, Lamotte O, Bourque S, Wendehenne D, Mazars C, Ranjeva R, Pugin A (2005) Proteinaceous and oligosaccharidic elicitors induce different calcium signatures in the nucleus of tobacco cells. Cell Calcium **38:** 527–538

Lecourieux D, Mazars C, Pauly N, Ranjeva R, Pugin A (2002) Analysis and effects of cytosolic free calcium increases in response to elicitors in *Nicotiana plumbaginifolia* cells. Plant Cell **14:** 2627–2641

Lecourieux D, Ranjeva R, Pugin A (2006) Calcium in plant defence-signalling pathways. New Phytol **171:** 249–269

Lee J, Klessig DF, Nürnberger T (2001) A harpin binding site in tobacco plasma membranes mediates activation of the pathogenesis-related gene HIN1 independent of extracellular calcium but dependent on mitogen-activated protein kinase activity. Plant Cell **13:** 1079–1093

Li J, Zhao-Hui C, Batoux M, Nekrasov V, Roux M, Chinchilla D, Zipfel C, Jones JD (2009) Specific ER quality control components required for biogenesis of the plant innate immune receptor EFR. Proc Natl Acad Sci USA **106:** 15973–15978

Liu Y, Schiff M, Marathe R, Dinesh-Kumar SP (2002) Tobacco RAR1, EDS1 and NPR1/NIM1 like genes are required for N-mediated resistance to tobacco mosaic virus. Plant J **30:** 415–429

Lorrain S, Vailleau F, Balagué C, Roby D (2003) Lesion mimic mutants: keys for deciphering cell death and defense pathways in plants? Trends Plant Sci **8:** 263–271

Lu D, Wu S, Gao X, Zhang Y, Shan L, He P (2010) A receptor-like cytoplasmic kinase, BIK1, associates with a flagellin receptor complex to initiate plant innate immunity. Proc Natl Acad Sci USA **107:** 496–501

Lu X, Tintor N, Mentzel T, Kombrink E, Boller T, Robatzek S, Schulze-Lefert P, Saijo Y (2009) Uncoupling of sustained MAMP receptor signaling from early outputs in an Arabidopsis endoplasmic reticulum glucosidase II allele. Proc Natl Acad Sci USA **106:** 22522–22527

Ludwig AA, Saitoh H, Felix G, Freymark G, Miersch O, Wasternack C, Boller T, Jones JD, Romeis T (2005) Ethylene-mediated cross-talk between calcium-dependent protein kinase and MAPK signaling controls stress responses in plants. Proc Natl Acad Sci USA **102:** 10736–10741

Ma W, Qi Z, Smigel A, Walker RK, Verma R, Berkowitz GA (2009a) Ca^{2+}, cAMP, and transduction of non-self perception during plant immune responses. Proc Natl Acad Sci USA **106:** 20995–21000

Ma W, Smigel A, Verma R, Berkowitz GA (2009b) Cyclic nucleotide gated channels and related signaling components in plant innate immunity. Plant Signal Behav **4:** 277–282

Malmström S, Askerlund P, Palmgren MG (1997) A calmodulin-stimulated Ca^{2+}-ATPase from plant vacuolar membranes with a putative regulatory domain at its N-terminus. FEBS Lett **400:** 324–328

Menke FL, van Pelt JA, Pieterse CM, Klessig DF (2004) Silencing of the mitogen-activated protein kinase MPK6 compromises disease resistance in *Arabidopsis*. Plant Cell **16:** 897–907

Miao Y, Laun TM, Smykowski A, Zentgraf U (2007) Arabidopsis MEKK1 can take a short cut: it can directly interact with senescence-related WRKY53 transcription factor on the protein level and can bind to its promoter. Plant Mol Biol **65:** 63–76

Miya A, Albert P, Shinya T, Desaki Y, Ichimura K, Shirasu K, Narusaka Y, Kawakami N, Kaku H, Shibuya N (2007) CERK1, a LysM receptor kinase, is essential for chitin elicitor signaling in Arabidopsis. Proc Natl Acad Sci USA **104:** 19613–19618

Mohr TJ, Liu H, Yan S, Morris CE, Castillo JA, Jelenska J, Vinatzer BA (2008) Naturally occurring nonpathogenic isolates of the plant pathogen *Pseudomonas syringae* lack a type III secretion system and effector gene orthologues. J Bacteriol **190:** 2858–2870

Mori IC, Schroeder JI (2004) Reactive oxygen species activation of plant Ca^{2+} channels: a signaling mechanism in polar growth, hormone transduction, stress signaling, and hypothetically mechanotransduction. Plant Physiol **135:** 702–708

Navarro L, Zipfel C, Rowland O, Keller I, Robatzek S, Boller T, Jones JD (2004) The transcriptional innate immune response to flg22: interplay and overlap with Avr gene-dependent defense responses and bacterial pathogenesis. Plant Physiol **135:** 1113–1128

Nekrasov V, Li J, Batoux M, Roux M, Chu ZH, Lacombe S, Rougon A, Bittel P, Kiss-Papp M, Chinchilla D, et al (2009) Control of the pattern-recognition receptor EFR by an ER protein complex in plant immunity. EMBO J **28:** 3428–3438

Nguyen HP, Chakravarthy S, Velásquez AC, McLane HL, Zeng L, Nakayashiki H, Park DH, Collmer A, Martin GB (2010) Methods to study PAMP-triggered immunity using tomato and *Nicotiana benthamiana*. Mol Plant Microbe Interact **23:** 991–999

Nühse TS, Bottrill AR, Jones AM, Peck SC (2007) Quantitative phosphoproteomic analysis of plasma membrane proteins reveals regulatory mechanisms of plant innate immune responses. Plant J **51:** 931–940

Nühse TS, Peck SC, Hirt H, Boller T (2000) Microbial elicitors induce activation and dual phosphorylation of the *Arabidopsis thaliana* MAPK 6. J Biol Chem **275:** 7521–7526

Ogasawara Y, Kaya H, Hiraoka G, Yumoto F, Kimura S, Kadota Y, Hishinuma H, Senzaki E, Yamagoe S, Nagata K, et al (2008) Synergistic activation of the Arabidopsis NADPH oxidase AtrbohD by Ca^{2+} and phosphorylation. J Biol Chem **283:** 8885–8892

Oh HS, Collmer A (2005) Basal resistance against bacteria in *Nicotiana benthamiana* leaves is accompanied by reduced vascular staining and suppressed by multiple *Pseudomonas syringae* type III secretion system effector proteins. Plant J **44:** 348–359

Peart JR, Cook G, Feys BJ, Parker JE, Baulcombe DC (2002) An EDS1 orthologue is required for N-mediated resistance against tobacco mosaic virus. Plant J **29:** 569–579

Petutschnig EK, Jones AM, Serazetdinova L, Lipka U, Lipka V (2010) The lysin motif receptor-like kinase (LysM-RLK) CERK1 is a major chitin-binding protein in Arabidopsis thaliana and subject to chitin-induced phosphorylation. J Biol Chem **285:** 28902–28911

Pugin A, Frachisse JM, Tavernier E, Bligny R, Gout E, Douce R, Guern J (1997) Early events induced by the elicitor cryptogein in tobacco cells: involvement of a plasma membrane NADPH oxidase and activation of glycolysis and the pentose phosphate pathway. Plant Cell **9:** 2077–2091

Ren D, Yang KY, Li GJ, Liu Y, Zhang S (2006) Activation of Ntf4, a tobacco mitogen-activated protein kinase, during plant defense response and its involvement in hypersensitive response-like cell death. Plant Physiol **141:** 1482–1493

Romeis T, Piedras P, Zhang S, Klessig DF, Hirt H, Jones JD (1999) Rapid Avr9- and Cf-9-dependent activation of MAP kinases in tobacco cell

cultures and leaves: convergence of resistance gene, elicitor, wound, and salicylate responses. Plant Cell **11:** 273–287

Saijo Y, Tintor N, Lu X, Rauf P, Pajerowska-Mukhtar K, Häweker H, Dong X, Robatzek S, Schulze-Lefert P (2009) Receptor quality control in the endoplasmic reticulum for plant innate immunity. EMBO J **28:** 3439–3449

Samuel MA, Hall H, Krzymowska M, Drzewiecka K, Hennig J, Ellis BE (2005) SIPK signaling controls multiple components of harpin-induced cell death in tobacco. Plant J **42:** 406–416

Samuel MA, Miles GP, Ellis BE (2000) Ozone treatment rapidly activates MAP kinase signalling in plants. Plant J **22:** 367–376

Seo S, Okamoto M, Seto H, Ishizuka K, Sano H, Ohashi Y (1995) Tobacco MAP kinase: a possible mediator in wound signal transduction pathways. Science **270:** 1988–1992

Sharma PC, Ito A, Shimizu T, Terauchi R, Kamoun S, Saitoh H (2003) Virus-induced silencing of WIPK and SIPK genes reduces resistance to a bacterial pathogen, but has no effect on the INF1-induced hypersensitive response (HR) in *Nicotiana benthamiana*. Mol Genet Genomics **269:** 583–591

Simon-Plas F, Elmayan T, Blein JP (2002) The plasma membrane oxidase NtrbohD is responsible for AOS production in elicited tobacco cells. Plant J **31:** 137–147

Small I (2007) RNAi for revealing and engineering plant gene functions. Curr Opin Biotechnol **18:** 148–153

Talke IN, Blaudez D, Maathuis FJ, Sanders D (2003) CNGCs: prime targets of plant cyclic nucleotide signalling? Trends Plant Sci **8:** 286–293

Tavernier E, Wendehenne D, Blein JP, Pugin A (1995) Involvement of free calcium in action of cryptogein, a proteinaceous elicitor of hypersensitive reaction in tobacco cells. Plant Physiol **109:** 1025–1031

Torres MA (2010) ROS in biotic interactions. Physiol Plant **138:** 414–429

Vinatzer BA, Teitzel GM, Lee MW, Jelenska J, Hotton S, Fairfax K, Jenrette J, Greenberg JT (2006) The type III effector repertoire of *Pseudomonas syringae* pv. *syringae* B728a and its role in survival and disease on host and non-host plants. Mol Microbiol **62:** 26–44

Wang H, Liu Y, Bruffett K, Lee J, Hause G, Walker JC, Zhang S (2008) Haplo-insufficiency of MPK3 in MPK6 mutant background uncovers a novel function of these two MAPKs in *Arabidopsis* ovule development. Plant Cell **20:** 602–613

Wang H, Ngwenyama N, Liu Y, Walker JC, Zhang S (2007) Stomatal development and patterning are regulated by environmentally responsive mitogen-activated protein kinases in *Arabidopsis*. Plant Cell **19:** 63–73

White PJ, Bowen HC, Demidchik V, Nichols C, Davies JM (2002) Genes for calcium-permeable channels in the plasma membrane of plant root cells. Biochim Biophys Acta **1564:** 299–309

Yoshioka H, Numata N, Nakajima K, Katou S, Kawakita K, Rowland O, Jones JD, Doke N (2003) *Nicotiana benthamiana* gp91phox homologs NbrbohA and NbrbohB participate in H_2O_2 accumulation and resistance to *Phytophthora infestans*. Plant Cell **15:** 706–718

Yuasa T, Ichimura K, Mizoguchi T, Shinozaki K (2001) Oxidative stress activates ATMPK6, an Arabidopsis homologue of MAP kinase. Plant Cell Physiol **42:** 1012–1016

Zhang J, Li W, Xiang T, Liu Z, Laluk K, Ding X, Zou Y, Gao M, Zhang X, Chen S, et al (2010) Receptor-like cytoplasmic kinases integrate signaling from multiple plant immune receptors and are targeted by a *Pseudomonas syringae* effector. Cell Host Microbe **7:** 290–301

Zhang J, Shao F, Li Y, Cui H, Chen L, Li H, Zou Y, Long C, Lan L, Chai J, et al (2007) A *Pseudomonas syringae* effector inactivates MAPKs to suppress PAMP-induced immunity in plants. Cell Host Microbe **1:** 175–185

Zhang S, Klessig DF (1998) The tobacco wounding-activated mitogen-activated protein kinase is encoded by SIPK. Proc Natl Acad Sci USA **95:** 7225–7230

Zipfel C, Kunze G, Chinchilla D, Caniard A, Jones JD, Boller T, Felix G (2006) Perception of the bacterial PAMP EF-Tu by the receptor EFR restricts Agrobacterium-mediated transformation. Cell **125:** 749–760

Zipfel C, Robatzek S, Navarro L, Oakeley EJ, Jones JD, Felix G, Boller T (2004) Bacterial disease resistance in Arabidopsis through flagellin perception. Nature **428:** 764–767